CMST 27(3) 129–136 (2021) DOI:10.12921/cmst.2021.0000019

The Monte Carlo Computer Experiment to Study the Order and Phase Transitions in the Mixed Phase Region Based on the Example of the 3D Ashkin-Teller Model

Z. Wojtkowiak, G. Musiał*

Adam Mickiewicz University
Faculty of Physics
ul. Uniwersytetu Poznańskiego 2
61-614 Poznań, Poland
**E-mail: gmusial@amu.edu.pl*

Received: 21 June 2021; accepted: 19 September 2021; published online: 28 September 2021

Abstract: In this paper, we demonstrate a new way of performing Monte Carlo (MC) simulations in a mixed phase region that is difficult to study, where with certain probabilities there are different ordering ways. That results in a large oscillation of the values of the computed thermodynamic quantities, which makes their interpretation very problematic. Our results are presented on the example of the 3D Askin-Teller (AT) model, where within a certain range of parameters with equal probabilities there are two different, but equivalent, ways of ordering two of the three order parameters showing independent behavior. The use of our new approach in an MC computer experiment allowed us to use Binder cumulant as well as Challa-and the Lee-Kosterlitz-like cumulants. This made it possible to locate phase transitions precisely enough to be able to use the energy distribution histogram method. According to the most effective strategy in the critical region we use our recently proposed cluster MC algorithm and the Metropolis algorithm beyond it, which are suitable for both the first-order and the continuous phase transitions in the 3D AT model. The new approach was demonstrated by determining smooth curves of magnetization and internal energy, and as a consequence by determining the location and character of the phase transition on the line between the mixed phase region and the paramagnetic phase.

Key words: mixed phase region, Monte Carlo computer experiment, phase transitions, lattice spin systems, 3D Ashkin-Teller model

I. INTRODUCTION

For several decades, the Ashkin-Teller (AT) model [1] has been one of the important points of reference in statistical physics, as it is a non-trivial generalization of the intensively used Ising model. After Fan [2] we express the AT model in terms of two standard Ising models put on the same lattice with spins s_i and σ_i at each lattice site i. Thus, we take into account only two spin interactions of a constant magnitude J_2 between the nearest neighbors. These two independent Ising models are coupled here by the four-spin interaction of a constant magnitude J_4, also only between couples of nearest neighboring spins. This leads to the effective Hamiltonian H

$$-\frac{H}{k_BT} = \sum_{[i,j]} \{K_2(s_i s_j + \sigma_i \sigma_j) + K_4 s_i \sigma_i s_j \sigma_j\}. \quad (1)$$

where $K_n = -J_n/k_BT$, with $n = 2$ or 4, $[i, j]$ denotes the summation over the nearest neighboring lattice sites. Moreover, k_B is the Boltzmann constant, and T is the temperature of the system. We consider here the symmetric 3D AT model, i.e., the one with the same interactions between s and σ spins, distributed in the cubic lattice.

Every year a dozen of works are devoted to it (see, e.g., the recent papers [3–7] and the ones cited therein), and it still finds new interesting applications, like recently for the modeling of the crystalline order in VO_2 [8], machine learning [9], the gapless Coulomb state [10], nanodomain patterns

in ultratetragonal $PbTiO_3$ [11], magnetic properties of nanotubes [12], and the elastic response of the DNA molecule to external force and torque [13]. This model is also very important from a theoretical point of view as there are some mappings between the AT model and other physical models [14].

The AT model is so attractive in terms of cognition and application as it is characterized by the $K_2(K_4)$ rich and complex phase diagram because not only two order parameters $\langle s\rangle$ and $\langle\sigma\rangle$ induce ordering, but also the product $\langle s\sigma\rangle$ exhibits independent ordering, where the symbol $\langle\ldots\rangle$ denotes the thermal average. The research done for this model and its applications can be found in many papers, e.g., [15–23].

A fragment of the phase diagram to which the results of our work relate is shown in Fig. 1. The first systematic study of the phase diagram of the 3D AT model on a cubic lattice was done by Ditzian et al. [24]. They exploited short series expansion and Monte Carlo (MC) simulations with very small samples, but they sketched the approximate phase diagram which is an important point of reference. For this reason, their results are ambiguous, mainly in the mixed phase region marked as "$\langle\sigma\rangle$" in Fig. 1. In the "$\langle\sigma\rangle$" region, either $\langle s\rangle$ or $\langle\sigma\rangle$ is ferromagnetically ordered but the other is not while $\langle s\sigma\rangle = 0$. Although few papers that relate to the "$\langle\sigma\rangle$" region have been published [20, 25, 26], their results are preliminary and this region still constitutes a real challenge.

In the phase diagram in Fig. 1 there are also the Baxter and paramagnetic (marked as "para") phases for which all order parameters, $\langle s\rangle$, $\langle\sigma\rangle$, and $\langle s\sigma\rangle$, are ferromagnetically ordered and are zero, respectively. For the phase marked as "$\langle s\sigma\rangle_{AF}$" $\langle s\rangle = \langle\sigma\rangle = 0$ and only the parameter $\langle s\sigma\rangle$ is antiferromagnetically ordered. The first-order phase transitions are denoted by the dotted curves, whereas the continuous ones are denoted by the solid curves. The labeled point positions are marked by $+$ and A, H, H', K, K' are the tricritical points. Arnold and Zhang [23] using MC simulations obtained the first more precise results along the line AP. Ising phase transitions occur along the continuous curve ending at the tricritical point K [21, 22, 27].

The 2D AT model shows the interesting line of continuously varying phase transitions at $K_4 \leq K_2$ first shown in the paper [28] and MC simulation results suggest the possibility of occurrence of nonuniversal behavior also in the 3D AT model [18, 20, 22, 24–26] but our recent results indicate only a wide crossover along the AH line and the rare coexistence of continuous and first-order phase transitions along the HH' line [18] shown in Fig. 1. It is noteworthy that the character of continuous phase transitions along the HK' line is still an open question.

The aim of our paper is to present a new method of performing an MC computer experiment to study the order and phase transitions between the mixed phase region "$\langle\sigma\rangle$" and the "para" phase on the example of the standard 3D AT model shown in Fig. 1. The "$\langle\sigma\rangle$" phase occurs only in the symmetric AT model in 3D. Due to the difficulty of obtaining unambiguous results and their interpretation, the "$\langle\sigma\rangle$" region is often omitted, as it is the most complex and the least recognized region of the 3D AT model phase diagram. To solve this problem, we have developed an appropriate strategy, precise tools such as three types of cumulants, and the energy distribution histogram, which enable a detailed analysis of this region. We have recently used these tools with success to analyze the first-order of phase transitions to the right of point A shown in Fig. 1 [15]. Due to the recently announced presence of metastable and unstable states [4], we use our cluster algorithm of the Wolff type [29] in the critical region and the Metropolis one beyond.

To illustrate the use of our method, we precisely determined the location of the phase transition and we determined its character for the point on the HK' line between the mixed phase region "$\langle\sigma\rangle$" and the paramagnetic phase shown in Fig. 1. These problems are important, topical and have not yet been solved in the bibliography of the subject.

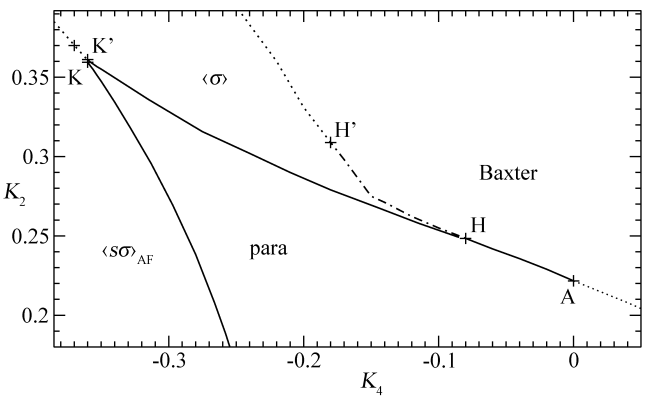

Fig. 1. A fragment of the phase diagram of the 3D AT model on a cubic lattice to which the results of our paper relate. The dotted curves denote the first order phase transitions, the solid ones stand for continuous transitions and the dotted-broken one indicates transitions of both types for different order parameters. In the phase labeled "Baxter" the system is ferromagnetically ordered with all order parameters $\langle s\rangle$, $\langle\sigma\rangle$ and $\langle s\sigma\rangle$ nonzero, whereas in the phase labeled "para" they all are zero. In the phase "$\langle s\sigma\rangle_{AF}$" there is $\langle s\rangle = \langle\sigma\rangle = 0$ and only the $\langle s\sigma\rangle$ is antiferromagnetically ordered. For the phase "$\langle\sigma\rangle$" called the mixed phase region $\langle s\sigma\rangle = 0$ and either $\langle s\rangle$ or $\langle\sigma\rangle$ is ferromagnetically ordered but the other is not. The positions of labeled points inside the phase diagram are marked by $+$ and A, H, H', K, K' are the tricritical points

II. THE APPLIED METHOD

To study the subject mixed phase region, we exploit the MC computer experiment with importance sampling of states and we consider the finite-size cubic samples of the lattice symmetric AT model, the behavior of which is fully determined by the Hamiltonian (1). These samples of size L^3 with periodic boundary conditions are sufficiently large to be able to compute the thermodynamic limit of our re-

sults. We perform our computer experiments to predict the equilibrium behavior of the 3D AT model according to the statistical mechanics methodology.

The detailed description of the MC computer experiment constructed by us for the 3D AT model based on the analysis of the dependencies of thermal averages of such thermodynamic variables as magnetization or internal energy, and three different cumulants on the coupling constant, and on the dependencies of the internal energy distribution histogram on energy can be found in our recent paper [15]. In this Section, apart from the computational aspects, we present only its key elements and we will focus primarily on explaining how to conduct it in the mixed phase region "$\langle\sigma\rangle$".

The specificity of such computer experiments of phase transitions in spin lattice systems with Ising's degrees of freedom is the necessity to execute hundreds, often even thousands of runs of programs, with the execution time ranging from several hours to many weeks for the systems with the largest size L^3 limited by the processing capabilities of the high-performance computers used [18, 22]. First, we bring our system to a state of thermodynamic equilibrium using the appropriate number of MC steps that we analyzed in our paper [29]. Moreover, in our MC computer experiments, in contrast to simple MC simulations, we not only compute thermodynamic quantities, but also carefully determine their error bars. For this purpose, one program run consists of the computation of 6 to 24 partial averages, each independently calculated from approximately 10^7 MC steps, but only every kth step contributes to the thermodynamic calculations ($6 < k < 10$), which is enough to avoid correlations between sampled configurations of our system using the Metropolis algorithm [29]. The problem of these correlations is radically smaller in the case of the cluster algorithm [30], which is also the case in our version of this algorithm [29].

Obviously, we get a true picture of the phase transition only in the thermodynamic limit. To obtain reliable extrapolations of our results to the thermodynamic limit, we perform computations in systems with the largest possible size L, which take many weeks at sequential processing. In order to get the results in a reasonable time using the MPI library, we have parallelized the processing in our computer experiments obtaining almost perfect speedup on symmetric multicomputers [31]. This is because communication between concurrently executing processes occurs only a few times: when broadcasting the original data by the master process, and when sending partial averages from slave processes to the master process. In the bibliography, there are other methods of parallelization of processing in cluster algorithms for models with degrees of freedom of the Ising type [32, 33], which rely on concurrent computations for newly added spins in a growing cluster performed on the GPU. As a result, the computing speed of the GPU for the 2D Ising model in the critical region is faster than the computing speed of the current processor core. However, conducting parallel calculations for newly added spins will not be optimal anymore [34], contrary to the parallelization of calculations of individual partial averages [31].

The presence of metastable and unstable states in the 3D AT model was recently signalized using the mean field method [4]. It is well known that the mean field theory is a solid tool, especially suitable for the first view of the problem, and it does not provide quantitative consistence with the precise results. Nevertheless, it gives a good qualitative insight into the problem [35]. So we generate equilibrium configurations of finite-size cubic spin samples for fixed values of our model parameters described above in the Hamiltonian (1) using our recently constructed cluster algorithm of the Wolff type [29] in the critical region and the Metropolis one beyond. This is the best strategy, also to optimize the time to obtain results with comparable uncertainties.

To prelocate a temperature-driven phase transition point, we fix a particular value of K_4 coupling and analyze Binder cumulant $Q_{\alpha,L}(K_2) = \langle M_\alpha^2\rangle_L^2/\langle M_\alpha^4\rangle_L$ dependences (see, e.g., [18, 21, 27, 36]), where $\langle M_\alpha^n\rangle_L$ denotes the n^{th} power of the order parameter α component, with $\alpha = s$, σ or their product $s\sigma$, which are averaged over an ensemble of independent samples of the size L^3. The lack of characteristic minima in the course of the $Q_{\alpha,L}(K_2)$ dependences indicates that the phase transition can be continuous [20, 36].

To check if there occurs the latent heat during a phase transition, i.e., to unambiguously determine the character of a phase transition and to more accurately determine the location of this transition point, we compute also the Challa [37]

$$V_{\alpha,L} = 1 - \frac{\langle E_\alpha^4\rangle_L}{3\langle E_\alpha^2\rangle_L^2} \tag{2}$$

and the Lee-Kosterlitz [38]

$$U_{\alpha,L} = \frac{\langle E_\alpha^2\rangle_L}{\langle E_\alpha\rangle_L^2} \tag{3}$$

like cumulants. Here $\langle E_\alpha^n\rangle_L$ is the n^{th} moment of the whole Hamiltonian ($\alpha = H$) or the interaction energy of α-degrees of freedom ($\alpha = s$, σ, or their product $s\sigma$) separately, which is averaged over an ensemble of independent samples of the size L^3. Thus, we are able to compute the latent heat l_α coming from each order parameter $\langle\alpha\rangle$ with $\alpha = s$, σ, or $s\sigma$ separately [18, 19, 22].

We analyze the dependences $V_{\alpha,L}(K_2)$ which show characteristic local minima $V_{\alpha,L}^{\min}$ [37] and $U_{\alpha,L}(K_2)$ characteristic local maxima $U_{\alpha,L}^{\max}$ [38] at a fixed value of K_4 coupling in the close critical region. When the thermodynamic limit $V_{\alpha,L}^{\min}$ value with its error bar remains different from 2/3 and the $U_{\alpha,L}^{\max}$ value with its error bar remains different from 1, we conclude that a phase transition is qualified to be of the first-order, otherwise we assume that the phase transition is continuous [18, 22, 37, 38]. The latent heat l_α coming from the whole Hamiltonian ($\alpha = H$) or the interac-

tion energy E_α of α order parameter in the thermodynamic limit

$$l_\alpha = E_{\alpha,+} - E_{\alpha,-}, \tag{4}$$

where $E_{\alpha,\pm} = E_\alpha(K_2 \to K_{2,c}|_\pm)$, are determined on the basis of the Lee-Kosterlitz formula [38, 39]

$$V_{\alpha,L}^{\min} = \frac{2}{3} - \frac{1}{12}\left(\frac{E_{\alpha,+}}{E_{\alpha,-}} - \frac{E_{\alpha,-}}{E_{\alpha,+}}\right)^2 + \frac{A_V}{L^3} \tag{5}$$

and using the method proposed in [22]. Eq. (5) was also obtained independently by Borgs, Kotecky, and Miracle-Sole [40] from a more rigorous point of view. $K_{2,c}$ in Eq. (5) is the critical value of K_2 coupling with the fixed value of K_4 and the quantity A_V stands for L independent expression of the complicated form [38]. Analogously, we can determine the latent heat l_α on the basis of the $U_{\alpha,L}$ cumulant maxima values scaled to the thermodynamic limit for each of the three α order parameters with $\alpha = s$, σ, or $s\sigma$ independently, as well as for the whole system ($\alpha = H$), using the Lee-Kosterlitz formula [38]

$$U_{\alpha,L}^{\max} = \frac{\left(E_{\alpha,+} + E_{\alpha,-}\right)^2}{4E_{\alpha,+}E_{\alpha,-}} + \frac{A_U}{L^3}, \tag{6}$$

where A_U stands for L independent complicated expression.

We conclude from Eqs. (5) and (6) that values and locations of cumulant $V_{\alpha,L}$ minima and of cumulant $U_{\alpha,L}$ maxima scale linearly versus L^{-3}. Using Eqs. (5) and (6) and the method proposed in [22] we can calculate the values of $E_{\alpha,+}$ and $E_{\alpha,-}$ and estimate the latent heat from Eq. (4). Moreover, the thermodynamic limit $K_{2,\alpha}^{\min}$ values of minima and $K_{2,\alpha}^{\max}$ values of maxima are far better estimations of the critical K_2 values than the preliminary ones obtained on the basis of the Binder cumulant $Q_{\alpha,L}(K_2)$ dependences.

Our method presented above [15] gives good results when the system has unambiguously determined equilibrium configurations of finite-size cubic spin samples for fixed values of our model parameters described above in the Hamiltonian (1).

However, in the mixed phase region, marked as "$\langle\sigma\rangle$" in Fig. 1, the situation is different: $\langle s\sigma\rangle = 0$ and there are two equally probable phases in which either $\langle s\rangle$ or $\langle\sigma\rangle$ is ferromagnetically ordered but the other is not in the thermodynamic limit. This causes the values of the computed thermodynamic quantities to oscillate as during sufficiently long simulations both phases will appear with approximately equal probability. Therefore, to obtain clear results we have worked out a new solution. We propose a conventional division of our system into two sublattices: the ordered one which will be marked with a capital letter Σ and the unordered one marked with a capital letter S. It is important that the decision to allocate the real spins σ and s to these conventional sublattices is decided only after each MCS is performed and the results from the spins with greater magnetization are systematically added to the results of the conventional sublattice Σ while the results from the second spins are added to the results of conventional sublattice S. The number of MCS must be large enough to compensate the separation of our system into these two artificial sublattices Σ and S in the paramagnetic region. Computations for the product of spins $s\sigma$ do not need to be changed.

We bear in mind that in the mixed phase region "$\langle\sigma\rangle$", two phases are equally probable in which either $\langle s\rangle$ or $\langle\sigma\rangle$ is ferromagnetically ordered but the other is not. In this situation, we introduce the conventional division into two sublattices, the first one with greater magnetization of Σ spins, and the second one with smaller magnetization of S spins. Thanks to this division, we get smooth dependences of thermodynamic quantities and of cumulant values on the coupling K_2 with a fixed value of the coupling K_4 for the analysis.

We have located phase transition point precisely enough to be able to use another independent method of checking for the presence of the latent heat during a phase transition with greater accuracy. We compute the probability $P_{\alpha,L}$ of the internal energy $E_{\alpha,L}$ appearance in the samples of finite size L^3. As in the case of cumulants, the $P_{\alpha,L}(E_{\alpha,L})$ values are computed independently for each degree of freedom $\alpha = s$, σ, or their product $s\sigma$, and also for the whole Hamiltonian (1) denoted by $\alpha = H$, at a critical value $K_{2,c}$. A characteristic histogram of the this energy E_α distribution with two peaks in the close critical region for first-order phase transitions can be observed [38, 41, 42]. The maxima of these peaks appear at the energy value $E_{\alpha,-,L}$ for the ordered state and at $E_{\alpha,+,L}$ for the unordered one for the samples of finite-size L. It is important that for continuous phase transitions only a single peak of the probability $P_{\alpha,L}(E_{\alpha,L})$ dependence appears in the thermodynamic limit. This is an additional clue for determining the character of a phase transition.

III. RESULTS AND CONCLUSIONS

We demonstrate our new way of performing MC computer experiments in the mixed phase region "$\langle\sigma\rangle$" shown in Fig. 1, where with equal probabilities there appear two different, but equivalent, ways of ordering two of the three order parameters: $\langle s\sigma\rangle = 0$ and either $\langle s\rangle$ or $\langle\sigma\rangle$ is ferromagnetically ordered but the other is not. To illustrate our method, we examine the phase transition for the point with $K_4 = -0.3$ lying on the HK' line, which is the boundary of the "$\langle\sigma\rangle$" region and the paramagnetic phase "para" shown in Fig. 2.

As we show below, we observe here that the values of characteristic local minima of the dependences $V_{\alpha,L}(K_2)$ and the values of characteristic local maxima of the dependences $U_{\alpha,L}(K_2)$ for $\alpha = \Sigma$, S, $s\sigma$, and H in the thermodynamic limit scale accordingly to the value $2/3$ for minima

and to 1 for maxima. This means that the transitions are continuous. Fig. 2 shows the dependence of the thermal average values of the square of magnetization $\langle M_\alpha^2\rangle_L$ for cubic samples of the finite size L^3 for all three order parameters with $\alpha = \Sigma$, S, and $s\sigma$ indicated in the legend. The vertical dotted line indicates the position of the phase transition point $K_{2,c} = 32905(30)$ estimated below. This figure also explains the reason for the occurrence of the minima of the cumulant $V_{\alpha,L}(K_2)$ dependences and of the maxima of the cumulant $U_{\alpha,L}(K_2)$ dependences also for $\alpha = S$ and $s\sigma$ for which we have a paramagnetic phase on both sides of the HK' line. The cumulant extremes for $\alpha = S$ and $s\sigma$ appear because in the critical region we observe non-zero magnetization, which, however, disappears as the size L increases, also shown in the legend, which is in line with expectations.

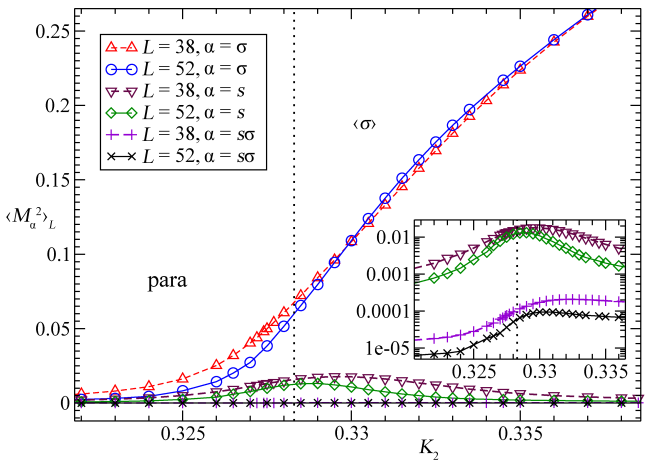

Fig. 2. The dependence of the thermal average values of the square of magnetization $\langle M_\alpha^2\rangle_L$ on the coupling K_2 for the fixed value of the four-spin interaction $K_4 = -0.3$. The inset shows the $\langle M_\alpha^2\rangle_L$ results for the order parameters $\langle\alpha\rangle$ with $\alpha = S$ and $s\sigma$, where the scale of the magnetization values is logarithmic. The values of the size L and items for α are explained in the legend. The vertical dotted line indicates the position of the phase transition point $K_{2,c} = 32905(30)$. The error bars are of the order of magnitude of symbols. Lines connecting the points have been drawn to guide the eye

From this introduction we can also see that at the beginning of the research it is necessary to determine the place of the phase transition marked with the vertical dotted line in Fig. 2. We obtain a preliminary estimation of the phase transition point from the intersections of the Binder cumulant [18, 21, 27, 36] curves $Q_{\alpha,L}(K_2)$ at the fixed value of the coupling $K_4 = -0.3$ presented in Fig. 3. This analysis has been performed for $\langle\Sigma\rangle$ order parameter, allowing us to estimate three to four decimal digits of the K_2 coupling critical value $K_{2,c} = 0.3274(18)$. Here $Q_{\Sigma,L}(K_2)$ curves intersect in such a way that for $L_1 < L_2$ at $K_2 < K_{2,c}$ one has $Q_{\Sigma,L_1} > Q_{\Sigma,L_2}$, while at $K_2 > K_{2,c}$ there appears $Q_{\Sigma,L_1} < Q_{\Sigma,L_2}$. The error bar should be estimated carefully here, as it is only an approximate indication of the critical region.

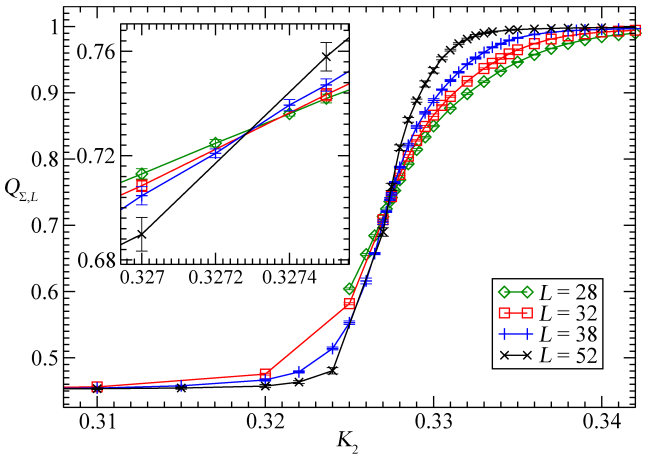

Fig. 3. The Binder cumulant $Q_{\Sigma,L}(K_2)$ dependences for the system size L values specified in the legend at the fixed value $K_4 = -0.3$. The inset shows the region in which these curves intersect. For clarity, the results for selected L values are presented. Lines connecting the points have been drawn to guide the eye

To check if there appears the latent heat during the phase transition and to improve the location of this transition point, we estimate the values and positions of cumulants $V_{\alpha,L}$ minima shown in Fig. 4 and of cumulants $U_{\alpha,L}$ maxima illustrated in Fig. 5 for degrees of freedom Σ ($\alpha = \Sigma$) or for the whole system ($\alpha = H$). To average the scatter of the results and to determine more precisely the ordinates of extrema $V_{\alpha,L}^{\min}$ and $U_{\alpha,L}^{\max}$ as well as their abscissas $K_{2,\alpha,L}^{\min}$ and $K_{2,\alpha,L}^{\max}$, our MC data were approximated by a polynomial of the third degree and marked by solid lines in Figs 4 and 5.

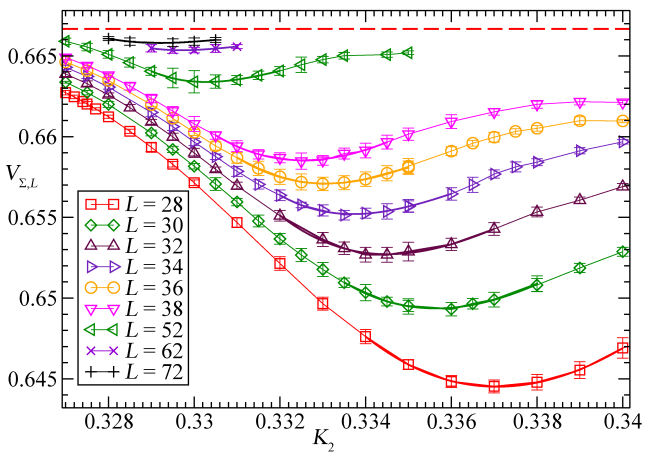

Fig. 4. The dependences $V_{\Sigma,L}(K_2)$ with characteristic local minima for system sizes L listed in the legend at the fixed value $K_4 = -0.3$. For clarity, the results for selected L values are presented. The horizontal dashed line indicates the limit 2/3 value. Lines connecting the points have been drawn to guide the eye

To estimate the value of the latent heat, we have exploited the Challa-like $V_{\alpha,L}$ and the Lee-Kosterlitz-like $U_{\alpha,L}$ cumulant properties explained in the previous section.

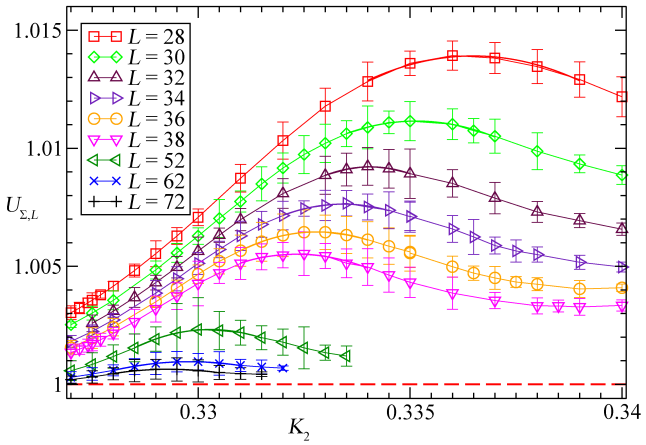

Fig. 5. The dependences $U_{\Sigma,L}(K_2)$ with characteristic local maxima for system sizes L listed in the legend at the fixed value $K_4 = -0.3$. For clarity, the results for selected L values are presented. The horizontal dashed line indicates the limit 1 value. Lines connecting the points have been drawn to guide the eye

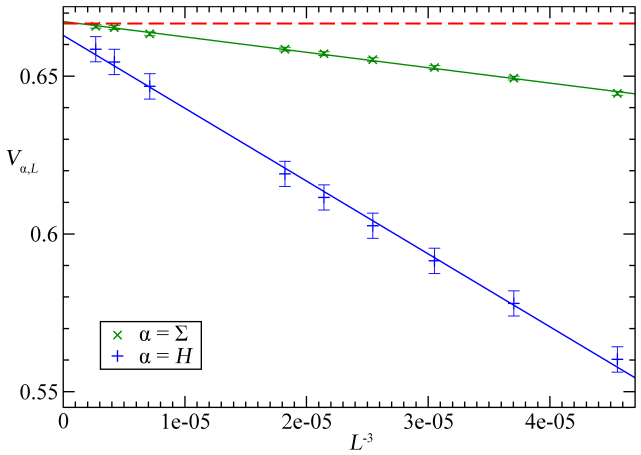

Fig. 6. The values of Challa-like cumulants minima $V^{\min}_{\alpha,L}$ for $\alpha = \Sigma$ and H extrapolated to the thermodynamic limit at the fixed value of the coupling $K_4 = -0.3$. The items α and symbols are explained in the legend. The dependences are fitted by straight solid lines using linear regression. The horizontal dashed line indicates the limit $2/3$ value

We have first calculated the values of the cumulant $V_{\alpha,L}$ minima and of the cumulant $U_{\alpha,L}$ maxima in the thermodynamic limit using linear regression for $V^{\min}_{\alpha,L}(L^{-3})$ and for $U^{\max}_{\alpha,L}(L^{-3})$ dependences with $\alpha = \Sigma$ and H, which follow from Eqs. (5) and (6), respectively. The analysis is illustrated in Fig. 6 for the Challa-like $V_{\alpha,L}$ cumulant and in Fig. 7 for the Lee-Kosterlitz-like $U_{\alpha,L}$ cumulant at the fixed value of the coupling $K_4 = -0.3$ for $\alpha = \Sigma$ and H indicated in the legend. The results of this extrapolation are $V^{\min}_{\Sigma,\infty} = 0.6673(8)$ and $V^{\min}_{H,\infty} = 0.663(5)$ as well as $U^{\max}_{\Sigma,\infty} = 0.9999(4)$ and $U^{\max}_{H,\infty} = 1.0017(24)$. One can see the clear linear character of our MC computer experiment data. There is the limit value $2/3$ within the cumulant $V^{\min}_{\alpha,\infty}$ values with their error bars and the limit value 1 within the cumulant $U^{\max}_{\alpha,\infty}$ values with their error bars in the thermodynamic limit for $\alpha = \Sigma$ and H. This means that the value of the latent heat here is zero.

Since for the conventional degrees of freedom Σ and S we have gathered contributions from both equally probable phases: this with $\langle\sigma\rangle$ nonzero and $\langle s\rangle = 0$ as well as with $\langle\sigma\rangle = 0$ and $\langle s\rangle$ nonzero, thus we have shown that the phase transition at the point with $K_4 = -0.3$ and $K_2 = 0.32905(30)$ is continuous.

Fig. 8 shows that the abscissas of the cumulant $V_{\Sigma,L}(K_2)$ dependences minima and the abscissas of the cumulant $U_{\Sigma,L}(K_2)$ dependences maxima within the limits of error bars in the thermodynamic limit scale to the same critical value $K_{2,c} = 0.32905(30)$. As the value of $K_{2,c}$, we have assumed the mean value of the Challa-like cumulant $K_{2,\Sigma,\infty,V} = 0.3290(3)$, and of the Lee-Kosterlitz-like cumulant $K_{2,\Sigma,\infty,U} = 0.3291(3)$. As shown in Fig. 8, these results are consistent with the preliminary estimation of $K_{2,\Sigma,\infty,Q} = 0.3274(18)$ obtained above using the Binder cumulant. Since we have obtained this $K_{2,c}$ value for the conventional degrees of freedom Σ and S, we conclude that

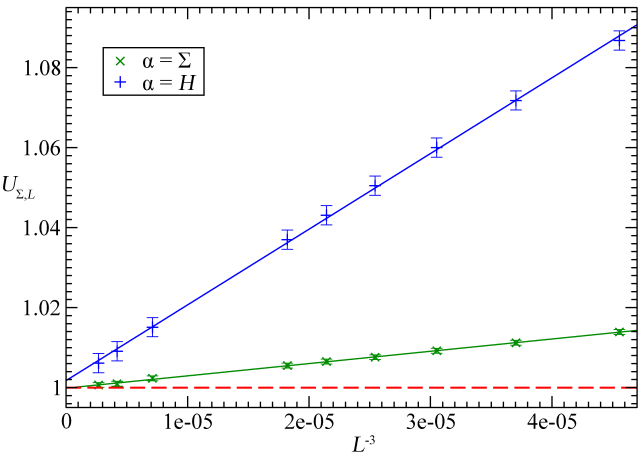

Fig. 7. The values of Lee-Kosterlitz-like cumulants maxima $U^{\max}_{\alpha,L}$ for $\alpha = \Sigma$ and H extrapolated to the thermodynamic limit at the fixed value of the coupling $K_4 = -0.3$. The items α and symbols are explained in the legend. The dependences are fitted by straight solid lines using linear regression. The horizontal dashed line indicates the limit 1 value

this is the phase transition point for both equally probable phases: the one with $\langle\sigma\rangle$ nonzero and $\langle s\rangle = 0$ as well as the second with $\langle\sigma\rangle = 0$ and $\langle s\rangle$ nonzero. We observe similar behavior along the entire HK'.

We have also computed the probability $P_{\alpha,L}$ of the internal energy $E_{\alpha,L}$ appearance in the samples of finite size L^3. As for cumulants, the $P_{\alpha,L}(E_{\alpha,L})$ values are computed independently for degrees of freedom $\alpha = \Sigma$, and also for the whole Hamiltonian (1) denoted by $\alpha = H$, at the calculated precisely enough critical value $K_{2,c} = 0.32905(30)$. The histogram of the this energy E_α distribution contains only one peak in the close critical region for $\alpha = \Sigma$ and H.

This is the independent confirmation that the phase transition is continuous.

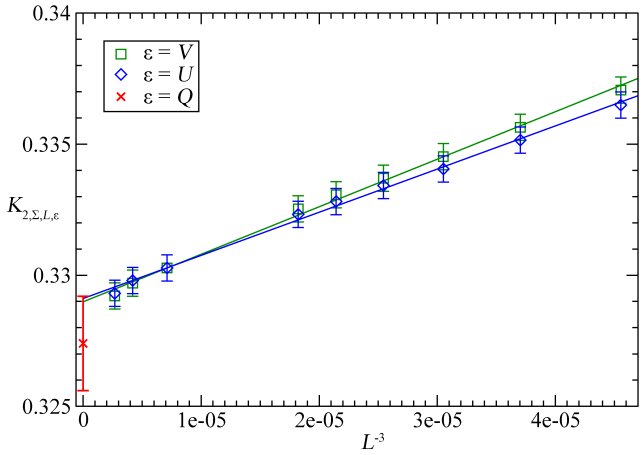

Fig. 8. Abscissas $K^{\min}_{2,\Sigma,L,V}$ of cumulants $V_{\Sigma,L}$ minima and $K^{\max}_{2,\Sigma,L,U}$ of cumulants $U_{\Sigma,L}$ maxima extrapolated to the thermodynamic limit at the fixed value of the coupling $K_4 = -0.3$. The symbols are explained in the legend. The dependences are fitted by straight solid lines using linear regression

In summary, we have demonstrated the way of performing our recently published MC experiments [15] in a mixed phase region that is difficult to study, as with certain probabilities there appear different ordering ways, which results in a large oscillation of the values of the computed thermodynamic quantities, which makes their interpretation very difficult. We have presented our method on the example of the point with $K_4 = -0.3$ on the boundary between the mixed phase region "$\langle\sigma\rangle$" and the paramagnetic one in the phase diagram of 3D AT model shown in Fig. 1. However, this method can be successfully applied to other spin lattice models whose phase diagram contains a mixed phase region. In the "$\langle\sigma\rangle$" region with equal probabilities there appear two different equivalent ways of ordering two of the three order parameters: $\langle s\sigma\rangle = 0$ and either $\langle s\rangle$ or $\langle\sigma\rangle$ is ferromagnetically ordered but the other is not.

Our concept to obtain clear results is based on that, there is a conventional division of our system into two sublattices. The ordered one which is marked with a capital Σ and the unordered one marked with a capital S. The decision to allocate the real spins σ and s to these conventional sublattices is decided only after each MCS is performed and the results from the spins with greater magnetization are systematically added to the results of conventional sublattice Σ while the results from the second kind of spins are added to the results of conventional sublattice S. We have controlled that the number of MCS is large enough to compensate the separation of our system into these two artificial sublattices Σ and S in the paramagnetic region.

Since for the conventional degrees of freedom Σ and S we have gathered contributions from both equally probable phases: this with $\langle\sigma\rangle$ nonzero and $\langle s\rangle = 0$ as well as with $\langle\sigma\rangle = 0$ and $\langle s\rangle$ nonzero, thus we have shown that the phase transition at the point with $K_4 = -0.3$ and $K_2 = 0.32905(30)$ is continuous.

In contrast to the results published so far in the bibliography, the implementation of our new approach in our MC experiment allowed us to use Binder cumulant, the Challa-like and the Lee-Kosterlitz-like cumulants, as well as the internal energy distribution histogram to obtain clear results a mixed phase region. According to the most effective strategy, in the critical region we have used our recently proposed cluster MC algorithm [29] and the Metropolis algorithm beyond the critical region, which are suitable for both, the first-order and continuous phase transitions in the 3D AT model.

Acknowledgment

Numerical calculations were carried out on the computing platforms of Poznań Supercomputing and Networking Center as well as the Faculty of Physics at Adam Mickiewicz University in Poznań.

References

[1] J. Ashkin, E. Teller, *Statistics of Two-Dimensional Lattices with Four Components*, Phys. Rev. **64**, 178 (1943).
[2] C. Fan, *On critical properties of the Ashkin-Teller model*, Phys. Lett. **39A**, 136 (1972).
[3] S.-P. Li, Z.-H. Sun, *Local and intrinsic quantum coherence in critical systems*, Phys. Rev. A **98**, 022317 (2018).
[4] J.P. Santos, J.A.J. Avila, D.S. Rosa, R.M. Francisco, *Multicritical phase diagram of the three-dimensional Ashkin-Teller model including metastable and unstable phases*, J. Magn. Magn. Mater. **469**, 35–39 (2019).
[5] G. Delfino, N. Lamsen, *Critical points of coupled vector-Ising systems. Exact results*, J. Phys. A: Math. Theor. **52**, 35LT02 (2019).
[6] P. Patil, A.W. Sandvik, *Hilbert space fragmentation and Ashkin-Teller criticality in fluctuation coupled Ising models*, Phys. Rev. B **101**, 014453 (2020).
[7] A. Benmansour, S. Bekhechi, B.N. Brahmi, N. Moussa, H. Ez-Zahraouy, *Monte Carlo study of thin magnetic Ashkin Teller films at the special point*, J. Magn. Magn. Mater. **511**, 166944 (2020).
[8] T. Lovorn, S.K. Sarker, *Complex Quasi-Two-Dimensional Crystalline Order Embedded in VO_2 and Other Crystals*, Phys. Rev. Lett. **119**, 045501 (2017).
[9] S.S. Lee, B.J. Kim, *Confusion scheme in machine learning detects double phase transitions and quasi-long-range order*, Phys. Rev. E **99**, 043308 (2019).
[10] G.-Y. Zhu, G.-M. Zhang, *Gapless Coulomb State Emerging from a Self-Dual Topological Tensor-Network State*, Phys. Rev. Lett. **122**, 176401 (2019).
[11] A. Kumar, J.G.M. Guy, L. Zhang, J. Chen, J.M. Gregg, J.F. Scott, *Nanodomain patterns in ultra-tetragonal lead titanate ($PbTiO_3$)*, Appl. Phys. Lett. **116**, 182903 (2020).
[12] R.M. Francisco, J.P. Santos, *Magnetic properties of the Ashkin-Teller model on a hexagonal nanotube*, Phys. Lett. A **383**, 1092–1098 (2019).
[13] C. Zhe, W. Ping, Z. Ying-Hong, *Ashkin-Teller Formalism for Elastic Response of DNA Molecule to External Force and Torque*, Commun. Theor. Phys. **49**, 525 (2008).
[14] M.E.J. Newman, G.T. Barkema, *Monte Carlo Methods in Statistical Physics*, Oxford University Press, Oxford (1999).

[15] G. Musiał, D. Jeziorek-Knioła, Z. Wojtkowiak, *Monte Carlo examination of first-order phase transitions in a system with many independent order parameters: Three-dimensional Ashkin-Teller model*, Phys. Rev. E **103**, 062124 (2021).
[16] J.P. Santos, F.C. Sá Barreto, *Upper Bounds on the Critical Temperature of the Ashkin-Teller Model*, Braz. J. Phys. **46**, 70–77 (2016).
[17] Ü. Akıncı, *Nonequilibrium phase transitions in isotropic Ashkin-Teller model*, Physica A **469**, 740–749 (2017).
[18] Z. Wojtkowiak, G. Musiał, *Wide crossover in the 3D Ashkin-Teller model*, Physica A **513**, 104–111 (2019).
[19] D. Jeziorek-Knioła, G. Musiał, Z. Wojtkowiak, *Arbitrarily Weak First Order Phase Transitions in the 3D Standard Ashkin-Teller Model by MC Computer Experiments*, Acta Phys. Polon. A **127**, 327 (2015).
[20] D. Jeziorek-Knioła, G. Musiał, L. Dębski, J. Rogiers, S. Dylak, *On Non-Ising Phase Transitions in the 3D Standard Ashkin-Teller Model*, Acta Phys. Polon. A **121**, 1105 (2012).
[21] G. Szukowski, G. Kamieniarz, G. Musiał, *Verification of Ising phase transitions in the three-dimensional Ashkin-Teller model using Monte Carlo simulations*, Phys. Rev. E **77**, 031124 (2008).
[22] G. Musiał, *Monte Carlo analysis of the tricritical behavior in a three-dimensional system with a multicomponent order parameter: The Ashkin-Teller model*, Phys. Rev. B **69**, 024407 (2004).
[23] P. Arnold, Y. Zhang, *Monte Carlo study of very weakly first-order transitions in the three-dimensional Ashkin-Teller model*, Nuclear Phys. B **501**, 803–837 (1997).
[24] R.V. Ditzian, J.R. Banavar, G.S. Grest, L.P. Kadanoff, *Phase diagram for the Ashkin-Teller model in three dimensions*, Phys. Rev. B **22**, 2542 (1980).
[25] G. Musiał, *A Monte Carlo study of the mixed phase region in the 3D Ashkin-Teller model*, Phys. Status Solidi B **236**, 486–489 (2003).
[26] G. Musiał, J. Rogiers, *On the possibility of nonuniversal behavior in the 3D Ashkin-Teller model*, Phys. Status Solidi B **243**, 335–338 (2006).
[27] G. Musiał, L. Dębski, G. Kamieniarz, *Monte Carlo simulations of Ising-like phase transitions in the three-dimensional Ashkin-Teller model*, Phys. Rev. B **66**, 012407 (2002).
[28] C. Fan, F.Y. Wu, *General Lattice Model of Phase Transitions*, Phys. Rev. B **2**, 723 (1970).
[29] Z. Wojtkowiak, G. Musiał, *Cluster Monte Carlo method for the 3D Ashkin-Teller model*, J. Magn. Magn. Mater. **500**, 166365 (2020).
[30] U. Wolff, *Collective Monte Carlo Updating for Spin Systems*, Phys. Rev. Lett. **62**, 361 (1989).
[31] G. Musiał, L. Dębski, *Monte Carlo Method with Parallel Computation of Phase Transitions in the Three-Dimensional Ashkin-Teller Model*, Lect. Notes in Comp. Sci. **2328**, 535–543 (2002).
[32] T. Preis, P. Virnau, W.Paul, J.J. Schneider, *GPU accelerated Monte Carlo simulation of the 2D and 3D Ising model*, J. Comput. Phys. **228**, 4468–4477 (2009).
[33] Y. Komura, Y. Okabe, *GPU-based single-cluster algorithm for the simulation of the Ising model*, J. Comput. Phys. **231**, 1209–1215 (2012).
[34] T.A. Kampmann, H.-H. Boltz, J. Kierfeld, *Parallelized event chain algorithm for dense hard sphere and polymer systems*, J. Comput. Phys. **281**, 864–875 (2015).
[35] G. Kamieniarz, R. Dekeyser, G. Musiał, L. Dębski, M. Bieliński, *Modified effective-field approach to low-dimensional spin-1/2 systems*, Phys. Rev. E **56**, 144 (1997).
[36] K. Binder, D.P. Landau, *Finite-size scaling at first-order phase transitions*, Phys. Rev. B **30**, 1477 (1984).
[37] M.S.S. Challa, D.P. Landau, K. Binder, *Finite-size effects at temperature-driven first-order transitions*, Phys. Rev. B **34**, 1841 (1986).
[38] J. Lee, J.M. Kosterlitz, *Finite-size scaling and Monte Carlo simulations of first-order phase transitions*, Phys. Rev. B **43**, 3265 (1991).
[39] K. Binder, *Applications of Monte Carlo methods to statistical physics*, Rep. Prog. Phys. **60**, 487 (1997).
[40] C. Borgs, R. Kotecky, S. Miracle-Sole, *Finite-size scaling for Potts models*, J. Stat. Phys. **62**, 529–551 (1991).
[41] D. Jeziorek-Knioła, Z. Wojtkowiak, G. Musiał, *Computation of Latent Heat based on the Energy Distribution Histogram in the 3D Ashkin-Teller Model*, Acta Phys. Polon. A **133**, 435–437 (2018).
[42] A. Billoire, T. Neuhaus, B.A. Berg, *A determination of interface free energies*, Nuclear Phys. B **413**, 795–812 (1994).

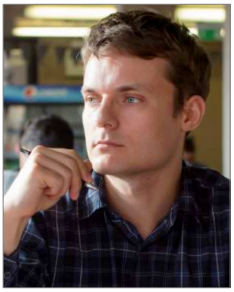

Zbigniew Wojtkowiak was born in 1989 in Śrem, Poland. He received his Master of Science degree in Biophysics in 2013 at the Adam Mickiewicz University in Poznań. From then on a PhD student at the same university in the Computational Physics Division. In his research he concentrates on numerical simulations and parallel Monte Carlo algorithms for classical spin systems. Together with Grzegorz Musiał, he applied the Wolff type cluster algorithm to the 3D Ashkin-Teller model for the first time. Moreover, he actively participates in the popularization of science during festivals and by conducting lessons in academic classes. He is author of 6 published scientific papers. Outside of science, he uses his analytical skills in various branches of business and industry.

Grzegorz Musiał was born in 1955 in Białożewin, Poland. He has got the Professor position at the Faculty of Physics, Adam Mickiewicz University in Poznań, Poland. In his research he joins physics and computing. Recently, his research work in physics has been concentrated mainly on many aspects of statistical physics in classical and quantum spin-lattice systems using numerical simulations. The computing research mainly concerns operating systems of the UNIX type and parallel computing in distributed environment, also with high heterogeneity. He is author of 70 published scientific papers and 5 books.